

Article

Effect of Fulvic Acid in Landfill Leachate Membrane Concentrate on Evaporation Process

Lu Liu¹, Mengyao Wu¹, Yuxiao Chen¹ and Heli Wang^{1,2,*}

¹ School of Water Resources and Environment, China University of Geosciences (Beijing), No. 29, Xueyuan Road, Haidian District, Beijing 100083, China

² Jiangsu Collaborative Innovation Center of Technology and Material of Water Treatment, Suzhou University of Science and Technology, Suzhou 215009, China

* Correspondence: wh15897@163.com; Tel.: +86-13801275897

Abstract: Landfill leachate membrane concentrate (LLMC) poses risks to the environment and is commonly treated by evaporation. As the main component of the dissolved organic matter in LLMC, fulvic acid (FA) was selected as a representative to investigate its effect on evaporation and the removal efficiency by pretreatment in this study. According to the water quality indexes and three-dimensional fluorescence spectra of LLMC samples collected from five landfills in China, the concentration of total organic carbon in LLMC was 700–2500 mg·L⁻¹, in which FA accounted for 50–85%. The boiling point and viscosity of the configured FA-NaCl-Na₂SO₄ solution both increased significantly when FA was concentrated 20 times (approximately 30,000 mg·L⁻¹). Due to the presence of FA, the violent frothing phenomenon appeared at above 70 °C in evaporation, and the solubility of CaSO₄·2H₂O in FA-NaCl-Na₂SO₄ solution was significantly lower than that without FA. All these results indicated that the high FA concentration in LLMC could lead to decreased heat transfer coefficient and evaporation capacity during evaporation. Therefore, the softening pretreatment including the addition of Ca(OH)₂, Na₂CO₃, and coagulants was employed to reduce the hardness and FA concentration. After the softening experiments, the removal efficiency of FA was >95% for the configured LLMC sample, while for the actual LLMC sample collected from landfills, the removal efficiency of FA and chemical oxygen demand could reach >80% and about 30%, respectively. The remaining concentration of FA in LLMC was about 200 mg·L⁻¹, and the recovery efficiency of clean water could be 90% in the evaporation process. This research has important guiding significance for the evaporation treatment of LLMC.

Keywords: landfill leachate membrane concentrate; fulvic acid; evaporation; softening; boiling point; viscosity



Citation: Liu, L.; Wu, M.; Chen, Y.; Wang, H. Effect of Fulvic Acid in Landfill Leachate Membrane Concentrate on Evaporation Process. *Processes* **2022**, *10*, 1592. <https://doi.org/10.3390/pr10081592>

Academic Editor: Adam Smoliński

Received: 20 June 2022

Accepted: 8 August 2022

Published: 12 August 2022

Publisher's Note: MDPI stays neutral with regard to jurisdictional claims in published maps and institutional affiliations.



Copyright: © 2022 by the authors. Licensee MDPI, Basel, Switzerland. This article is an open access article distributed under the terms and conditions of the Creative Commons Attribution (CC BY) license (<https://creativecommons.org/licenses/by/4.0/>).

1. Introduction

By the end of 2020, about 99.32% of municipal solid wastes (MSW) in China have been harmlessly treated by landfill, incineration, composting, and other methods with a total capacity of 897,700 tons·day⁻¹ [1], of which landfill treatment accounts for 55%. Due to the living habits of Chinese residents, the water content of MSW is relatively high, basically above 50% [2]. The leachate generated accounts for 35–50% and 25–35% of the landfill volume during landfill disposal and incineration disposal, respectively. In summary, 1 ton of MSW will produce 0.25–0.5 m³ of leachate throughout the landfill disposal process.

Landfill leachate is a highly contaminated liquid that contains high levels of inorganic ions, organic matter, and other toxics, such as heavy metals, ammonia, and emerging organic contaminants (EOCs) [3]. Its composition is related to hydrogeological conditions, climate and garbage components, and especially to the age of the landfill [4]. Depending on the age of the landfill, garbage degradation can be divided into five stages, namely, the aerobic stage, the anaerobic acid stage, the initial methanogenic stage, the stable

methanogenic stage, and the humic decomposition stage [5]. Accordingly, the produced landfill leachate can be divided into three main categories: young (from the aerobic stage and anaerobic acid stage), intermediate (from the initial methanogenic stage), and old (from the stable methanogenic stage and the humic decomposition stage) [6]. With the increase of the landfill's age, the pH value of the leachate changes from acidic to weakly alkaline, the content of ammonia nitrogen ($\text{NH}_4^+\text{-N}$) increases, and the concentration of chemical oxygen demand (COD) and biodegradability gradually decrease. The leachate characteristics at different ages are summarized in Table 1 [7–10].

Table 1. Characteristics of the landfill leachate at different ages ^a.

Phase	Age (Year)	pH [7]	COD _{cr} (mg·L ⁻¹)	BOD ₅ /COD [8]	TOC/COD [8]	Ammonia [9,10] (mg·L ⁻¹)
Young	<5	<6.5	6000–60,000	0.5–1	<0.3	<400
Intermediate	5–10	6.5–7.5	4000–10,000	0.2–0.5	0.3–0.5	400–1500
Old	>10	>7.5	1000–6000	<0.2	>0.5	>1500

^a TOC: total organic carbon; BOD₅: five-day biochemical oxygen demand; COD: chemical oxygen demand; COD_{cr}: chemical oxygen demand by potassium dichromate method.

Standalone biological treatments generally fail to meet discharge standards because of their ineffectiveness in degrading biologically refractory organic matter. To overcome this limitation, biological treatments are often combined with MBR (membrane bio-reactor), NF (nanofiltration), and RO (reverse osmosis) processes. The combined processes can reduce COD, ammonia nitrogen, chrome, and toxic substances of leachate by about 88%, 95%, >99.9%, and >99.9%, respectively [11]. For leachate that is poorly biodegradable, a two-stage DTRO (disk-tube reverse osmosis) unit is often adopted. As the most commonly used method for treating landfill leachate in recent decades, membrane-based techniques exhibit some outstanding features, such as small occupation areas, high volume loading, good effluent quality, and high disinfection capability. However, some critical operations, such as pretreatment, fouling, chemical cleaning, and replacement of the membrane module of membrane-based techniques, are complicated, expensive, and rigorous. When the membrane unit produces the up-to-standard effluent, the 25–50% concentrated solution is also produced. The membrane cannot degrade the pollutants including organic pollutants, inorganic salts, ammonia-nitrogen, heavy metals, and EOCs, but can concentrate them into a smaller volume [12–17]. Therefore, the landfill leachate membrane concentrate (LLMC) contains large amounts of refractory pollutants and saline compounds, posing risks to the surrounding soil, groundwater, surface water, and human health.

Current treatment methods of LLMC include recirculation to landfills [18], advanced oxidation [19–21], coagulation sedimentation [22,23], electrodialysis [24], adsorption [25], membrane distillation [26], and evaporation [17]. According to the characteristics of LLMC, to meet the Chinese standard (GB/T 31962-2015) [27], and solve the problem of salt in LLMC, evaporation is commonly used. However, during the evaporation treatment of actual LLMC, as the solution continues to concentrate, the evaporation system faces operational challenges due to the high concentration of organic and inorganic substances. The increase of boiling point (BP), viscosity change, scaling, and blockage of the evaporator will all lead to a decrease in the heat transfer coefficient and production capacity of the evaporator. The frothing of organic components will bring small liquid droplets out from the LLMC, leading to the increase of COD content in the effluent. Considering that evaporation has been highly matured in the inorganic salt chemical industry, the difficulty in evaporation treatment of LLMC is probably attributed to these highly refractory organic substances. Dissolved organic matter (DOM) in LLMC can be categorized into three main types: humic acid (HA), fulvic acid (FA), and a hydrophilic component (HyI). Among these, the recalcitrant HA and FA constitute the majority of DOM [28]. Previous research revealed that the humic substances (HA and FA) account for 83.3% of TOC in LLMC, and FA accounts for 40–75% of TOC [29,30].

However, current studies on evaporation processes mainly focus on the seawater desalination and zero discharge of industrial high-salinity water [31–34]. The most important

thermal distillation processes are multistage flash, multi-effect distillation, and mechanical vapor recompression [35]. In order to reduce the energy consumption of pure thermal processes, technologies such as membrane distillation, humidification-dehumidification, and adsorption desalination have been developed [36]; most studies have focused on how to improve the efficiency of the evaporation system in the treatment of highly saline water. However, there are few studies on the evaporation process of the organics-salt mixed system.

In this study, FA was selected as the representative substance of DOM in LLMC, and the effect of FA on evaporation was investigated through a series of experiments, and the removal efficiency of FA in the pretreatment of LLMC was further studied. The purposes of this study are to (1) reveal the effect of FA on the evaporation process, (2) clarify the FA removal efficiency and pretreatment mechanism, and (3) provide guidance for the pretreatment and evaporation treatment of LLMC.

2. Materials and Methods

2.1. Samples

The actual (real-life) LLMC samples were collected from the Beijing Beitiantang landfill, Nanjing Niushoushanshuige landfill, Xiangtan Shuangma landfill, Hengyang landfill, and Shijiazhuang Nantaihang landfill in July 2021. The basic information about each landfill site is tabulated in Table 2. The landfills sampled are located in different regions in China. The landfill types include young, intermediate, and old landfills. Hence, the characteristics of collected samples are highly representative.

Table 2. Basic information on the sampling landfills.

Age	Region	Basic Info	Leachate Treatment ^a	Concentrate Treatment
3 years	Xiangtan, Hunan	the third landfill area started in 2018	two-stage biological treatment + UF + NF + RO	recirculation
7 years	Shijiazhuang, Hebei	started in 2014	pretreatment + two-stage DTRO	recirculation
10 years	Beijing	started in 2012	two-stage biological treatment + UF + NF + RO	built LLMC treatment system in 2018
10 years	Hengyang, Hunan	started in 2012	two-stage biological treatment + UF + NF + RO	recirculation
Closure	Nanjing, Jiangsu	closed in 2014	two-stage biological treatment + UF + NF + RO	recirculation

^a MBR: membrane bio-reactor, NF: nanofiltration, RO: reverse osmosis, DTRO: disk-tube reverse osmosis; UF: ultrafiltration (line 68), BP: boiling point (line 75), PAC: polyaluminum chloride, PAM: polyacrylamide, DOM: dissolved organic matter.

To investigate the effect of FA in evaporation, the configured (laboratory-made) LLMC samples were prepared in the laboratory with the reagent (fulvic acid, FA > 90%, the melting point of FA is 246 °C) purchased from Shanghai McLean Biochemical Technology Co., Ltd. (Shanghai, China).

2.2. Characterization

COD and ammonia were measured by a multi-parameter bench photometer (DR2800, HACH, Loveland, CO, USA). The pH value was measured using a portable pH meter (FE20, METTLER TOLEDO, Columbus, OH, USA). Conductivity was measured using a conductivity meter (HQ2200, HACH, USA). Samples were filtered through a 0.45 µm filter membrane (Tianjin Jinteng Laboratory Equipment Co., Tianjin, China), and their TOC was measured using a TOC analyzer (TOC-5000A, Shimadzu, Kyoto, Japan). The concentrations of Ca²⁺, Mg²⁺, SO₄²⁻, and Cl⁻ were analyzed by ion chromatography (930Compact, Metrohm, Herisau, Switzerland). The concentration of FA was determined by an ultraviolet-visible spectrophotometer with a wavelength of 254 nm [37]. Since the fluorescence spectroscopy allows qualitative and semi-quantitative analysis of DOM [38],

the three-dimensional (3D) fluorescence spectrometer (F-6500, Hitachi, Japan) was used to analyze the type and fraction of DOM in the LLMC, which can also verify the ultraviolet light analysis results.

The BP and viscosity of samples were measured by an oil bath (DF101, Shijihuayu, Beijing, China) and a digital viscometer (NDJ-5S, Shanghai Yueping, China), respectively.

2.3. Evaporation Test

During evaporation, large organic molecules are difficult to volatilize or remove, thus they are continuously concentrated in the evaporator. According to the FA concentration of actual LLMC and the recovery efficiency of 85–95% in evaporation (the maximum concentration factor is 20 times), FA was configured at concentrations of 500–30,000 mg·L⁻¹ with the concentration gradient of 500, 2500, 5000, 6500, 10,000, 15,000, 20,000, 25,000, and 30,000 mg·L⁻¹. The BP, viscosity, and saturated solubility of CaSO₄·2H₂O under different FA concentrations were measured. At the same time, to simulate the actual LLMC in the evaporation system, a saturated concentration of NaCl-Na₂SO₄ mixed salt (salt mass content is 30%) was added into the above FA solutions. The salts concentration in the final solution is shown in Supplementary Materials. The saturated NaCl-Na₂SO₄ solution was prepared based on the phase equilibrium data of the water-salt system according to a previous report [39], that is, the mass fractions of NaCl and Na₂SO₄ in the solution at 100 °C were 25.25% and 4.51%, respectively. For the newly configured FA-NaCl-Na₂SO₄ solutions, their BP, viscosity, and saturated solubility of CaSO₄·2H₂O were measured.

BP was determined when the temperature inside the flask remained unchanged during the boiling process. Viscosity was measured by a digital viscometer. The static equilibrium method was used to determine the saturated solubility of CaSO₄·2H₂O at different temperatures. Firstly, CaSO₄·2H₂O powder was added into the FA solution to reach saturation. Then, the solution was heated to 50, 60, 70, 80, and 90 °C by a rotary evaporator (DZFY-2L, Kexing, China) to sufficiently dissolve the CaSO₄·2H₂O for 3 h and remained at this temperature for 30–60 min. Afterwards, the supernatant was sampled and filtered through a 0.45 µm membrane, followed by measuring the Ca²⁺ concentration in the supernatant to determine the saturated solubility of CaSO₄·2H₂O. The experiments were performed two times, and the results were averaged with the error of lower than 0.3%.

2.4. Softening Experiment

Due to the high hardness of the LLMC, softening pretreatment should be employed to reduce a sustainable amount of the hardness ions before the evaporation process. Therefore, batch softening tests were conducted to analyze the FA removal efficiency. Four configured samples with FA concentrations of 500, 1000, 1500, and 2000 mg·L⁻¹ were used based on the FA concentration in actual LLMC. The selected actual LLMC originated from the Xiangtan landfill and Shijiazhuang landfill by nanofiltration and reverse osmosis, respectively. LLMC is a high-hardness and low-alkalinity wastewater, which is different from the membrane concentrate produced from garbage incineration landfills. In this case, the combined agents of Ca(OH)₂ and Na₂CO₃ were used as softening agents [40], and PAC and PAM were also added to reduce precipitation time. Afterwards, the softening experiment was completed by stirring at ambient temperature for a total reaction time of 120 min. The removal efficiency of FA in the pretreatment process was analyzed by the concentration of COD and FA in the effluent.

3. Results and Discussion

3.1. LLMC Characteristics

The actual LLMC sample collected from the Nantaihang landfill in Shijiazhuang was a two-stage DTRC concentrate, while the other samples were nanofiltration (NF) concentrates. All actual LLMC samples were dark brown liquids with obvious odor. Their water quality indexes are shown in Table 3.

Table 3. Characteristics of LLMC.

Indicators	Xiangtan, Hunan	Shijiazhuang, Hebei	Beijing	Hengyang, Hunan	Nanjing, Jiangsu
pH	7.41	7.13	7.03	7.99	7.16
Ammonia nitrogen, mg·L ⁻¹	2560	2780	1560	2420	2560
COD _{cr} , mg·L ⁻¹	5320	3400	1900	2770	5480
BOD ₅ /COD	0.18	0.2	0.08	0.19	0.09
TOC, mg·L ⁻¹	2365	1250	705	1946	1991
FA, mg·L ⁻¹	1635	975	587	980	1378
FA/TOC, wt. %	69.13%	78.00%	83.26%	50.31%	69.21%
EC, ms/cm	65.5	53.9	47.8	22.6	13.13
Ca ²⁺ , mg·L ⁻¹	547.6	605	681.7	410.7	665.6
Mg ²⁺ , mg·L ⁻¹	713.3	207	536.7	240.8	398.4
TH, mg·L ⁻¹	4341.8	2375	3940.5	2030.08	3324
Cl ⁻ , mg·L ⁻¹	8624	9765	9552	6153	2417
SO ₄ ²⁻ , mg·L ⁻¹	954	658	468.8	490.3	227

LLMC is generally known for its high salt content, most of which are chlorides and sulfates; it contains 2000–10,000 mg·L⁻¹ chloride and 200–1000 mg·L⁻¹ sulfate, resulting in conductivity of 13–66 mS/cm. The concentrations of calcium and magnesium in LLMC are high, equal to 400–600 mg·L⁻¹ and 200–700 mg·L⁻¹, respectively, leading to a total hardness of more than 2000 mg·L⁻¹ (calculated as CaCO₃). If evaporated directly without pretreatment, CaCO₃, Mg(OH)₂, and CaSO₄ will be concentrated to saturation, separated from the solution, and form a scale in the evaporator. Therefore, it is essential to integrate an effective softening pretreatment unit before the evaporation system.

As shown in Table 1, after biological treatment (aerobic and anaerobic) in the previous stage, the COD and TOC in LLMC are 200–6000 mg·L⁻¹ and 700–2500 mg·L⁻¹, respectively. Refractory FA has a concentration of 500–1500 mg·L⁻¹ and is the main component of TOC, accounting for 50–85%. The BOD₅/COD ratios of LLMC are less than 0.2, which means that LLMC is virtually non-biodegradable. The results of the 3D fluorescence spectra of the actual LLMC samples from four landfills in Figure 1 and the control samples (configured solutions with different FA concentrations) in Figures S1–S4 in the Supplementary Materials draw the same conclusions. The strong peak areas located in EM400–500 and EX225–275 in Figure 1a indicate that the main organic matter in LLMC of the Beijing landfill is FA. The strong peak areas located in EM400–500, EX225–275, and EX300–400 in Figure 1b,c indicate that the main organic matters in LLMC of the Hengyang landfill and Nanjing landfill are FA and HA. The strong peak areas located in EM400–500 and EX320–380 in Figure 1d indicate that the main organic matter in LLMC of the Xiangtan landfill is HA.

During evaporation, the refractory organic matters in the LLMC will be further concentrated [41]. When LLMC is concentrated 20 times, the FA concentration can reach 30,000 mg·L⁻¹. Thus, the effect of a large amount of FA on evaporation needs to be further studied.

3.2. Effect of FA on Evaporation Parameters

3.2.1. Effect of FA on BP and Viscosity

According to the heat transfer rate equations in the Supplementary Materials, the increase of BP and viscosity in evaporation will have a significant influence on the evaporation efficiency.

According to Equation (S1) in the Supplementary Materials, when BP rises significantly, the effective heat transfer temperature difference of the heat exchanger decreases [42], which leads to a decrease in the heat transfer rate and the evaporation of the waste liquid at the same flow rate, thus consuming more energy. Viscosity is an important hydrodynamic property of wastewater, which affects the heat transfer coefficient according to Equations (S2)–(S9) in the Supplementary Materials [43]. The liquid is not easily evaporated at high viscosity, which results in a significant increase in the evaporation time and energy

consumption. Therefore, the effect of FA concentration on BP and viscosity was analyzed in this study. According to the analysis of actual LLMC samples in Table 1, the configured concentration of FA was 500–30,000 mg·L⁻¹ to simulate the water quality of the concentrate obtained from 20 times the concentration from evaporation. At the same time, the saturated NaCl-Na₂SO₄ solution was added to the above-mentioned FA solution to investigate the variation of BP and viscosity of the FA-NaCl-Na₂SO₄ mixed system. The results are shown in Figures 2 and 3.

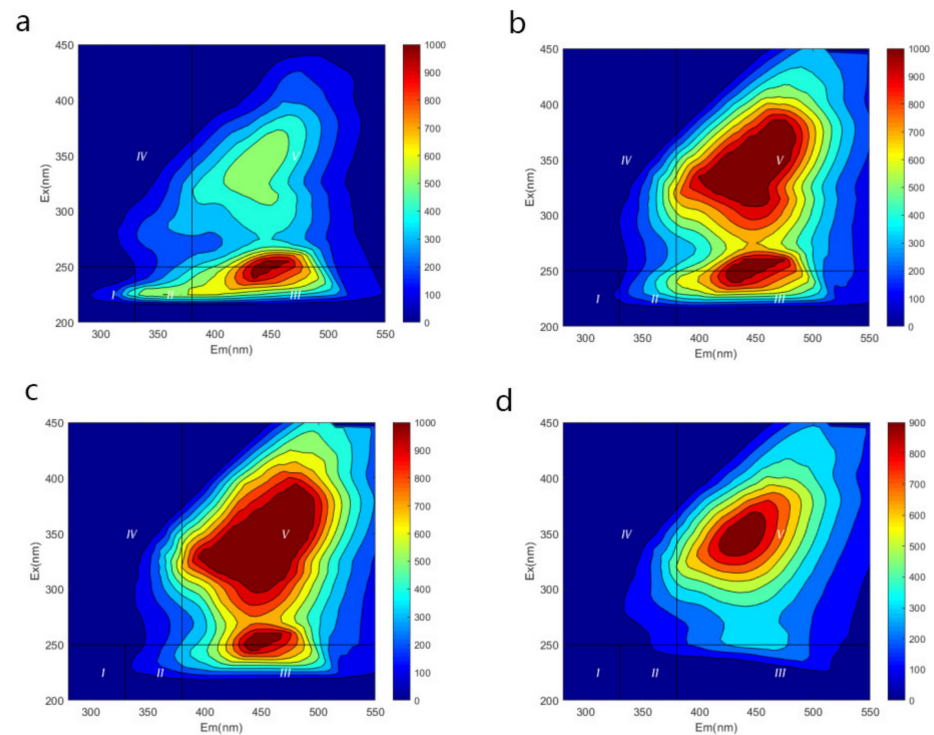


Figure 1. Three-dimensional fluorescence spectra of LLMC from (a) Beijing Beitiantang landfill, (b) Hengyang landfill, (c) Nanjing Shuige landfill, and (d) Xiangtan Shuangma landfill.

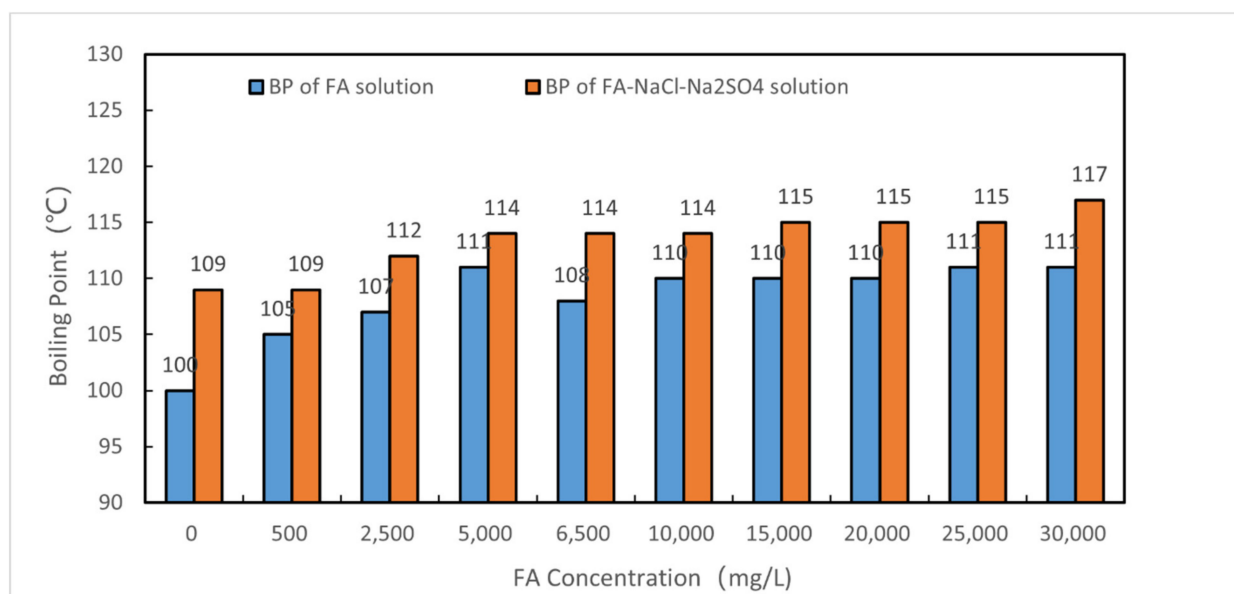


Figure 2. Boiling point variation in FA solution and FA-NaCl-Na₂SO₄ solution.

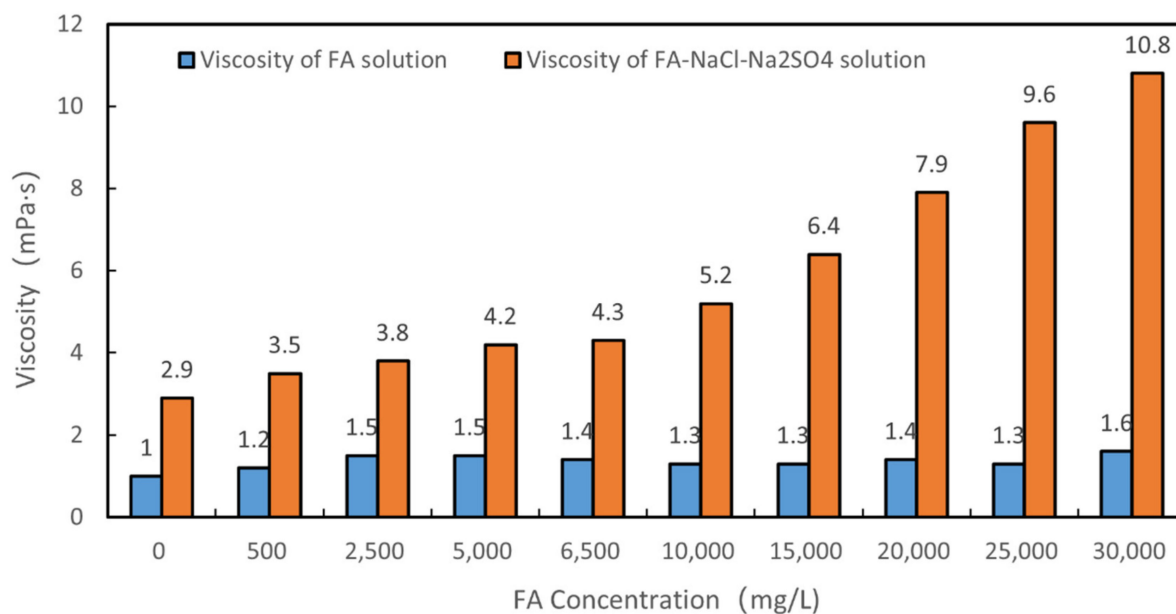


Figure 3. Viscosity variation in FA solution and FA-NaCl-Na₂SO₄ solution at 28 °C.

Figure 2 indicates that BP continued to rise with increasing FA concentrations. In the FA solution, the BP rises were about 8–10 °C at the FA concentration of 500–30,000 mg·L⁻¹ compared to pure water. In the FA-NaCl-Na₂SO₄ solution, the highest BP rise was increased by 17 °C compared to pure water, higher than that of the single FA solution. The temperature of secondary steam in practical application is about 15–20 °C [44]. If the BP rise of the inlet liquid is too high, the heat transfer efficiency will be decreased due to the limited capacity of a single compressor, while the use of a multi-stage compressor requires complex system and operation management. Considering the effective heat transfer temperature difference and heat loss, liquid with BP rise higher than 12 °C is generally difficult to evaporate. Therefore, during the evaporation of LLMC, when the FA concentration is higher than 2500 mg·L⁻¹, it is difficult to evaporate the solution with a single compressor due to the high BP rise caused by organics and salt.

According to Figure 3, due to the existence of FA, the viscosity of the FA solution is higher than that of pure water, and the viscosity was 1.2–1.6 cP at the ambient temperature of 28 °C. For the FA-NaCl-Na₂SO₄ solution, its viscosity increased significantly with the increase of FA concentration, and its viscosity was 3.5–11 cP, much higher than that of pure water and saturated brine (25% NaCl and 5% Na₂SO₄ solution, at 20 °C) [39]. Combining Equations (S2)–(S5) in Supplementary Materials, it can be inferred that the heat transfer coefficient of LLMC during evaporation will be lower than that of the salt solution due to the existence of FA.

3.2.2. Effect of FA on Frothing Phenomenon

In the relevant experiments in Section 3.2.1, the frothing phenomenon occurred in heating the FA solution and the FA-NaCl-Na₂SO₄ solution. The frothing will cause pollutants to splash into steam and deteriorate the effluent quality. Since the evaporation temperature and soluble component are key factors in determining the frothing strength of liquids, boiling experiments were carried out with FA concentrations of 500, 600, 700, 1000, 1200, 1500, 2000, 2500, 5000, 6500, 10,000, 15,000, 20,000, 25,000, and 30,000 mg·L⁻¹. In the evaporation process of the FA solution and the FA-NaCl-Na₂SO₄ solution, the frothing phenomenon appeared at above 70 °C, and the frothing phenomenon became more obvious with the increase of the FA concentration. For the single FA solution, a lot of organic matter splashed during frothing at FA concentration higher than 5000 mg·L⁻¹. For the FA-NaCl-Na₂SO₄ solution, a lot of organic matter was sprayed out of the Erlenmeyer flask during frothing

at the FA concentration of above $2000 \text{ mg}\cdot\text{L}^{-1}$. Figure 4a,b show the photos of frothing phenomena in these experiments.

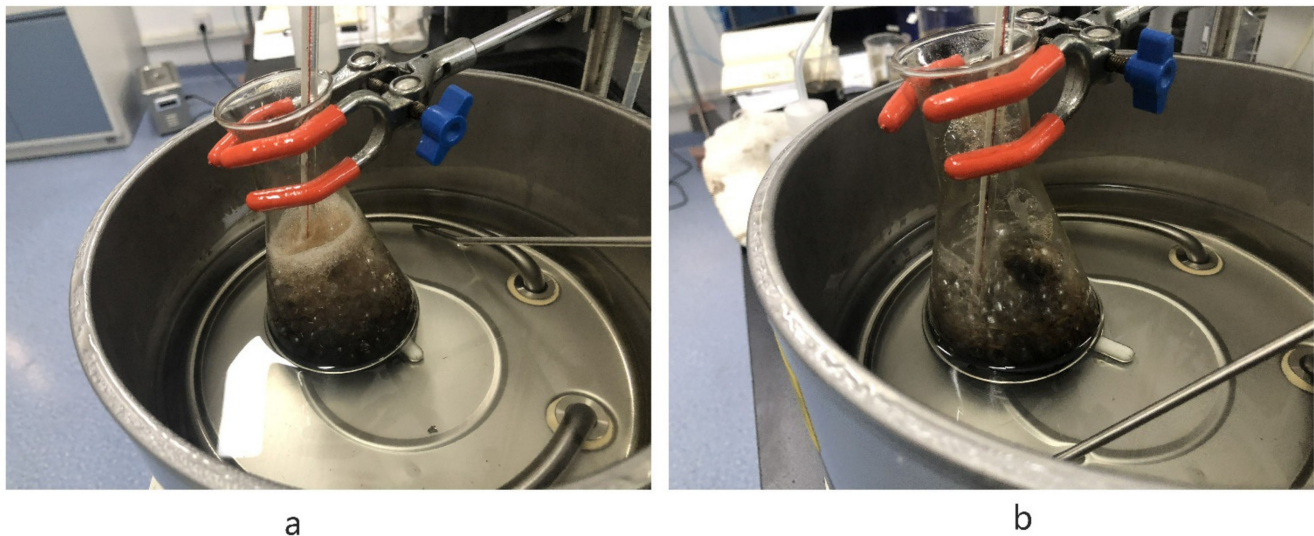


Figure 4. Photos of sudden frothing of (a) $5000 \text{ mg}\cdot\text{L}^{-1}$ FA solution and (b) $2000 \text{ mg}\cdot\text{L}^{-1}$ FA NaCl- Na_2SO_4 solution at $70 \text{ }^\circ\text{C}$.

3.2.3. Effect of FA on the Solubility of Calcium Sulfate

The calcium scale produced during evaporation mainly includes calcium carbonate and calcium sulfate. When the calcium carbonate scale is formed, it can react and be removed by immersing in 1–3% hydrochloric acid [45]. The evaporation efficiency of an evaporator can return to normal after a short cleaning process, which does not affect the normal production. In contrast, the formation of the calcium sulfate scale is irreversible and difficult to remove by common chemical cleaning. It is necessary to prevent calcium sulphate scaling, and the scaling trend can be predicted through saturation calculation. Therefore, the effect of FA on the calcium sulfate scale in the evaporation system can be estimated by the maximum calcium concentration of the influent. The solubility curves of $\text{CaSO}_4\cdot 2\text{H}_2\text{O}$ at different FA concentrations and temperatures are shown in Figure 5.

As depicted in Figure 5, when the temperature is constant, the saturated solubility of $\text{CaSO}_4\cdot 2\text{H}_2\text{O}$ first decreases and then increases with the increase of FA concentration. When the FA concentration was $500\text{--}10,000 \text{ mg}\cdot\text{L}^{-1}$, the saturated solubility of $\text{CaSO}_4\cdot 2\text{H}_2\text{O}$ decreased with the FA concentration and was lower than that in pure water. When the FA concentration was $10,000\text{--}30,000 \text{ mg}\cdot\text{L}^{-1}$, the saturated solubility of $\text{CaSO}_4\cdot 2\text{H}_2\text{O}$ increased and was higher than that in pure water. The reason can be explained as follows: when the FA concentration is relatively low (i.e., $<10,000 \text{ mg}\cdot\text{L}^{-1}$), calcium ions and sulfate ions are ionized after the dissolution of calcium sulfate in water, and unstable hydrated calcium ions and hydrated sulfate ions are formed by combining water molecules through intermolecular force and electrostatic interaction [46]. However, the hydrophilic group [47] in the FA structure competes with the above hydrated ions for water molecules in the solvent, which will reduce the concentration of calcium sulfate. Moreover, FA is a relatively stable natural macromolecular organic matter with an intermittent network of sparse aromatic rings. There are many holes of different sizes in the structure [48], resulting in high reaction activity and high adsorption capacity [49]. Some calcium ions will be adsorbed by FA, leading to a decreased concentration of dissolved calcium ions. At higher FA concentrations, i.e., greater than $10,000 \text{ mg}\cdot\text{L}^{-1}$, the attraction of polar functional groups [50] contained in FA to solute will overcome the binding force between ions of solute molecules, resulting in the formation and dissolution of complexes and more dissolved calcium ions. At the same FA concentration, when the temperature rose from 50 to $90 \text{ }^\circ\text{C}$, the solubility of $\text{CaSO}_4\cdot 2\text{H}_2\text{O}$ decreased slightly with the increase in temperature. According to the

above data, the water hardness and inflow conditions before evaporation should be set scientifically.

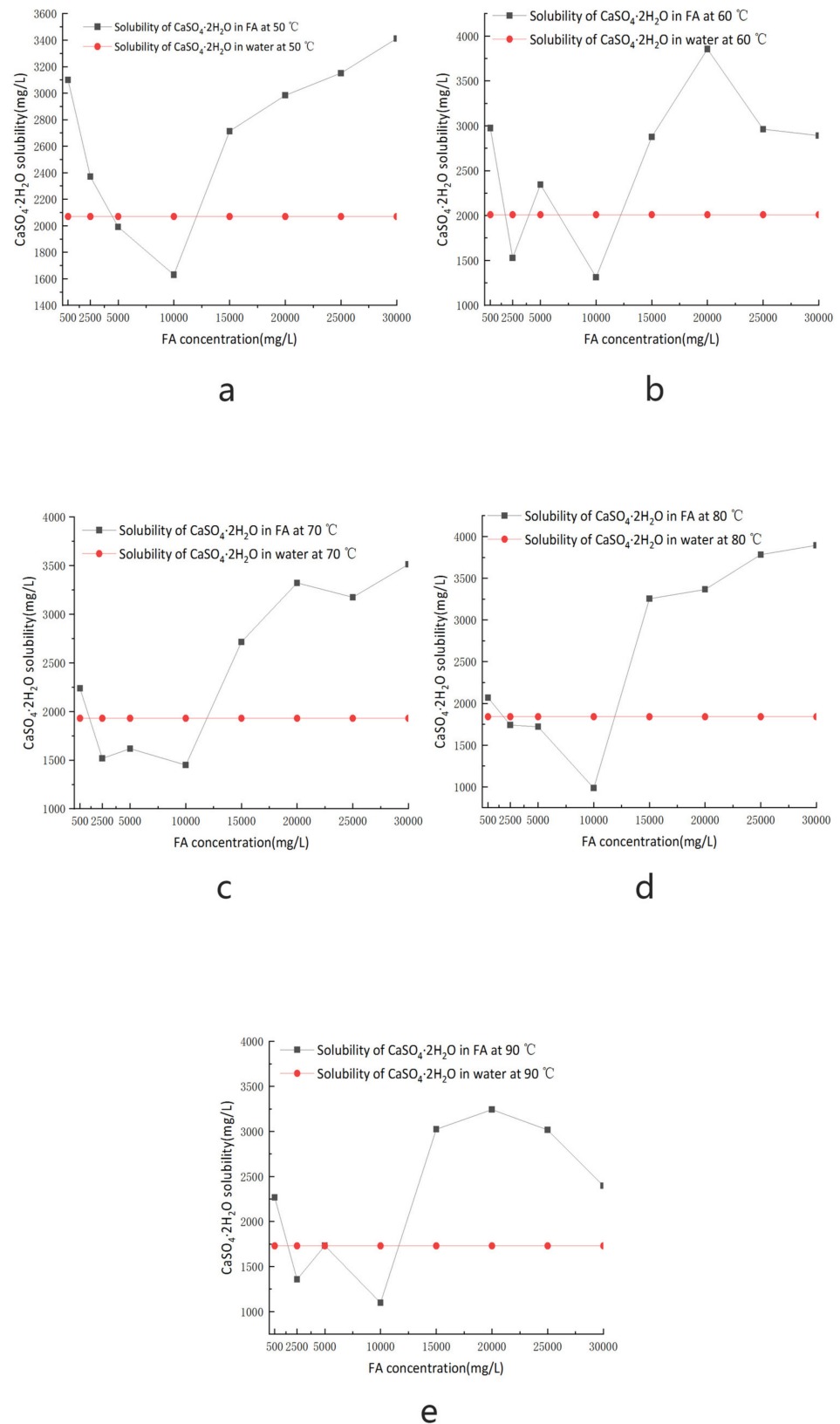


Figure 5. Saturated solubility of $\text{CaSO}_4 \cdot 2\text{H}_2\text{O}$ at different temperatures and FA concentrations. (a) 50 °C, (b) 60 °C, (c) 70 °C, (d) 80 °C, and (e) 90 °C.

The solubility of $\text{CaSO}_4 \cdot 2\text{H}_2\text{O}$ in the $\text{NaCl-Na}_2\text{SO}_4\text{-H}_2\text{O}$ system has been well studied previously. J. Block et al. [51], L.B. Yeatts et al. [52], and F.K. Cameron et al. [53] measured the solubility of $\text{CaSO}_4 \cdot 2\text{H}_2\text{O}$ in $\text{NaCl-Na}_2\text{SO}_4$ solution at 25–100 °C, and their data were similar. Comparing the solubility data in these literatures [50–53], it can be seen that the solubility of $\text{CaSO}_4 \cdot 2\text{H}_2\text{O}$ in $\text{FA-NaCl-Na}_2\text{SO}_4$ solution is lower than that in $\text{NaCl-Na}_2\text{SO}_4$ solution (about $4.5 \text{ g}\cdot\text{L}^{-1}$ at the salt concentration of 30%), which is due to the existence of FA.

In summary, when FA is concentrated 20 times (approximately $30,000 \text{ mg}\cdot\text{L}^{-1}$), the BP and viscosity of the $\text{FA-NaCl-Na}_2\text{SO}_4$ solution will increase significantly and the solubility of $\text{CaSO}_4 \cdot 2\text{H}_2\text{O}$ will decrease compared with that without FA, resulting in decreased evaporation capacity and increased energy consumption. Therefore, when the evaporation process is adopted, pretreatment should be employed to reduce organics concentration to a sustainable value. The FA concentration is suggested to be lower than $2000 \text{ mg}\cdot\text{L}^{-1}$ to improve the stability of evaporators and the quality of effluent.

3.3. Removal Efficiency of FA in the Softening Process

3.3.1. Removal Efficiency of FA of Configured Solutions

The removal efficiency of FA in the softening pretreatment process was investigated. In the actual process of coagulation and sedimentation, the dosage is generally controlled by adjusting the pH value to >11 . In fact, when the pH value is greater than 11, both calcium and magnesium ions were removed by hydrolysis to form precipitates [54]. Table 4 shows the compositions of the inlet and outlet liquids during the softening process.

Table 4. Treatment results of configured samples after the softening process.

Initial Parameters		After Adding $\text{Ca}(\text{OH})_2$				After Adding Na_2CO_3			
pH ^a	FA Concentration ($\text{mg}\cdot\text{L}^{-1}$)	$\text{Ca}(\text{OH})_2$ ($\text{mg}\cdot\text{L}^{-1}$)	FA Concentration ($\text{mg}\cdot\text{L}^{-1}$)	Ca^{2+} ($\text{mg}\cdot\text{L}^{-1}$)	Removal Efficiency of FA	pH ^a	FA Concentration ($\text{mg}\cdot\text{L}^{-1}$)	Ca^{2+} ($\text{mg}\cdot\text{L}^{-1}$)	Removal Efficiency of FA
7.18	500	0.4661	23.04	503	91%	12.44	10.52	17	96%
7.23	1000	0.6544	38.77	738	92%	12.46	17.39	58	97%
7.42	1500	0.5931	57.01	922	93%	12.22	30.67	76.5	96%
7.53	2000	0.6213	68.98	1093	93%	12.2	42.61	116	96%

^a pH values before the addition of Na_2CO_3 .

As shown in Table 4, the $\text{FA-NaCl-Na}_2\text{SO}_4$ solution is a neutral solution with an initial pH value of about 7.5. FA may be significantly removed in the softening process due to the adsorption of calcium ions under alkaline conditions by various active groups and spatial structures of FA. The removal efficiency of FA was 91–93% after adding $\text{Ca}(\text{OH})_2$, while the removal efficiency of FA after adding Na_2CO_3 was much higher (96–97%). This is due to the coprecipitation [55] between the generated CaCO_3 precipitates and FA, which further improves the removal efficiency of FA.

After sedimentation for two hours, the amount of produced sludge from the solutions with FA concentrations of 500, 1000, 1500, and 2000 $\text{mg}\cdot\text{L}^{-1}$ were 10, 20, 28, and 39 mL, respectively. The initial volumes were 170 mL, 170 mL, 200 mL, and 200 mL respectively. Hence, the percentages of sludge produced volumes were 5.9%, 11.8%, 14%, and 19.5%. Figure 6 shows the photos of the sedimentation results. The main components of chemical sludge are CaCO_3 , $\text{Mg}(\text{OH})_2$, and some coprecipitation organic pollutants, which need to be dewatered and then landfilled.

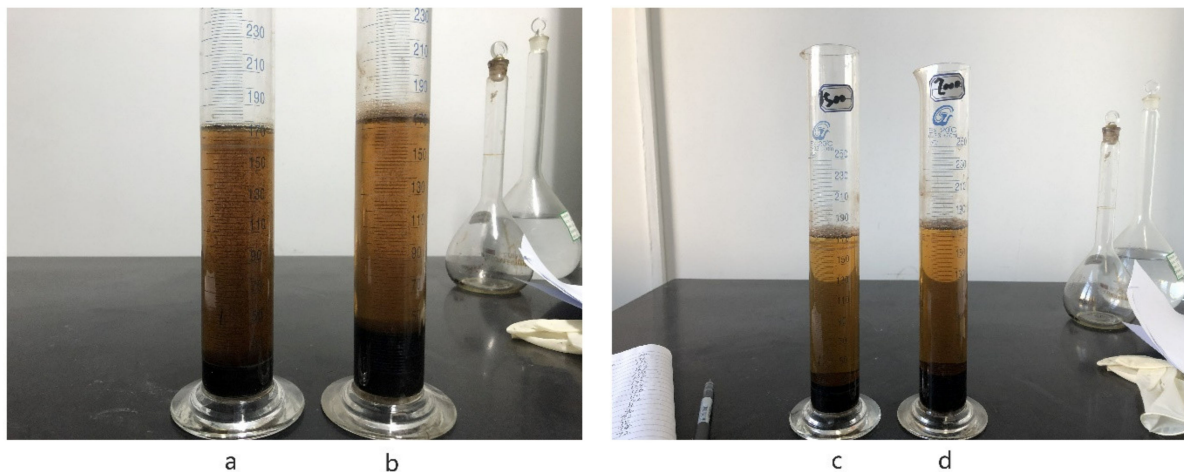


Figure 6. Sludge photos after sedimentation with FA concentrations of (a) 500, (b) 1000, (c) 1500, and (d) 2000 mg·L⁻¹.

3.3.2. Removal Efficiency of FA of Actual LLMC Samples

The removal efficiency of FA in the softening process using actual LLMC samples was tested. For the actual LLMC sample from the Xiangtan landfill with the volume of 170 mL, 5.8 g of Ca(OH)₂ was firstly added to adjust the pH value to 12, and then 9.03 g of Na₂CO₃ was added to react with the calcium ions to form precipitation. After that, PAC and PAM were added with the optimal dosage of 2 mg L⁻¹ and 0.01 mg L⁻¹, respectively. Finally, the water quality of the supernatant was measured after settling for 120 min. The same procedures were followed when testing the 170 mL Shijiazhuang sample, and the dosages of Ca(OH)₂ and Na₂CO₃ were changed to 2.6 and 4.5 g, respectively. The water quality results of the above softening process are shown in Table 5.

Table 5. Treatment results of actual LLMC samples after the softening process.

Landfill	Indicator	Influent Concentration	Effluent Concentration	Removal Efficiency
Xiangtan	COD _{cr} , mg·L ⁻¹	5320	3674	30.9%
	FA, mg·L ⁻¹	1635	258.1	84%
	EC, μs/cm	65,500	547	99.2%
	Ca ²⁺ , mg·L ⁻¹	547.6	98	82.1%
	Mg ²⁺ , mg·L ⁻¹	713.3	43	93.7%
	TH, mg·L ⁻¹	4341.08	424.17	90.2%
Shijiazhuang	COD _{cr} , mg·L ⁻¹	3400	2320	31.8%
	FA, mg·L ⁻¹	975	187	80.8%
	EC, μs/cm	53,900	495	99%
	Ca ²⁺ , mg·L ⁻¹	605	11	98.2%
	Mg ²⁺ , mg·L ⁻¹	207	6.12	97%
	TH, mg·L ⁻¹	2375	53	97.8%

As can be seen from Table 4, when the pH was adjusted to 12, the hardness ions could be significantly removed. For the actual LLMC sample from the Xiangtan landfill, the removal efficiencies of calcium ions, magnesium ions, and total hardness were 82.1%, 93.7%, and 90.2%, respectively, while those for the Shijiazhuang sample were 98.2%, 97%, and 97.8%, respectively. Meanwhile, the removal efficiencies of COD and FA were 30.9% and 84% for the Xiangtan sample and 31.8% and 80.8% for the Shijiazhuang sample, respectively. These results indicate that the softening pretreatment has good removal efficiency for macromolecular FA but limited removal efficiency for small molecular organic pollutants [28]. This is because the softening agents have different removal effects on organic matters with different molecular weights.

The FA remaining in LLMC after the softening process was approximately $200 \text{ mg}\cdot\text{L}^{-1}$. When this liquid is concentrated 20 times during the evaporation process, the FA concentration will be greater than $4000 \text{ mg}\cdot\text{L}^{-1}$, leading to the BP rise of $14 \text{ }^\circ\text{C}$ and the viscosity of $>4 \text{ cP}$. Furthermore, when the operating temperature is above $70 \text{ }^\circ\text{C}$, the frothing phenomenon will occur. Therefore, it is difficult to reduce the volume of the liquid by 95% using evaporation. By reducing the recovery of clean water in the evaporation process to 90%, the operational stability of the evaporator will be improved, but the evaporation efficiency will be reduced.

Furthermore, conducting a future study on the effect of evaporation parameters such as temperature, pH, and concentration on effluent quality and evaporation efficiency is recommended.

4. Conclusions

To avoid the environmental threats of LLMC and solve the problem in evaporation caused by high organic content, FA was selected as a representative to investigate its effect on evaporation, and the softening pretreatment-evaporation process was employed in this study. LLMC samples collected from five landfills in different regions of China were characterized by their water quality indexes and 3D fluorescence spectra, which showed that FA accounted for 50–85% of DOM in LLMC, and the predominant DOM in LLMC of the Beijing landfill was FA. Evaporation tests showed that the presence of FA resulted in a significant increase of BP, and the BP rise was $>10 \text{ }^\circ\text{C}$ at the FA concentration of $2500 \text{ mg}\cdot\text{L}^{-1}$. With the increase of FA concentration, the viscosity of the FA-NaCl- Na_2SO_4 solution increased and the violent frothing phenomenon appeared at above $70 \text{ }^\circ\text{C}$ in evaporation. In addition, the $\text{CaSO}_4\cdot 2\text{H}_2\text{O}$ solubility in the FA-NaCl- Na_2SO_4 solution was lower than that without FA. All these results indicated that high FA concentration in LLMC could lead to increased energy consumption, decreased evaporation capacity and deteriorated effluent quality. Therefore, it was suggested that the pretreatment should be employed to reduce the FA concentration to $<1500 \text{ mg}\cdot\text{L}^{-1}$ before evaporation. The softening pretreatment included the addition of $\text{Ca}(\text{OH})_2$, Na_2CO_3 , and coagulants in this study. When the FA concentration varied from 500 to 2000 mg/L, the removal efficiency of FA for the configured LLMC sample was $>95\%$ in 120 min. For the softening pretreatment with the actual LLMC sample collected from landfills, the removal efficiency of FA and COD could reach $>80\%$ and about 30%, respectively. After that, the FA remaining in the LLMC was about $200 \text{ mg}\cdot\text{L}^{-1}$, and the recovery efficiency of clean water could reach 90% in the subsequent evaporation process. This study is of great guiding significance for the engineering design of LLMC softening-evaporation treatment, and challenges for applying it in actual LLMC treatment including the scale-up issue remain unclear, which will be studied in future work.

Supplementary Materials: The following are available online at <https://www.mdpi.com/article/10.3390/pr10081592/s1>, Figure S1: 3D fluorescence spectra of the configured $500 \text{ mg}\cdot\text{L}^{-1}$ FA solution. (III) FA with the proportion of 46.39%, (V) HA with the proportion of 19.97%; Figure S2: 3D fluorescence spectra of the configured $1000 \text{ mg}\cdot\text{L}^{-1}$ FA solution. (III) FA with the proportion of 49.0%, (V) HA with the proportion of 16.35%; Figure S3: 3D fluorescence spectra of the configured $1500 \text{ mg}\cdot\text{L}^{-1}$ FA solution. (III) FA with the proportion of 49.13%, (V) HA with the proportion of 16.37%; Figure S4: 3D fluorescence spectra of the configured $2000 \text{ mg}\cdot\text{L}^{-1}$ FA solution. (III) FA with the proportion of 49.03%, (V) HA with the proportion of 16.27% [56–58].

Author Contributions: Conceptualization, L.L.; investigation, L.L., M.W., and Y.C.; resources, H.W.; writing—original draft, L.L. and M.W.; writing—review and editing, L.L. and H.W. All authors have read and agreed to the published version of the manuscript.

Funding: This research received no external funding.

Institutional Review Board Statement: Not applicable.

Informed Consent Statement: Not applicable.

Data Availability Statement: The data presented in this study are available in the figures and tables.

Conflicts of Interest: The authors have no relevant financial or non-financial interests to disclose.

References

1. The Ministry of Ecology and Environment of the People's Republic of China. *The Bulletin on the State of China's Ecological and Environment in 2020*; State Council of China: Beijing, China, 2020. (In Chinese)
2. Zhuang, Y. Current situation and management countermeasures of municipal solid waste treatment technology. *Eng. Technol. Res.* **2020**, *13*, 279–280.
3. Yu, X.; Sui, Q.; Lyu, S.; Zhao, W.; Liu, J.; Cai, Z.; Yu, G.; Barcelo, D. Municipal solid waste landfills: An underestimated source of PPCPs in the water environment. *Environ. Sci. Technol.* **2020**, *54*, 9757–9768. [[CrossRef](#)] [[PubMed](#)]
4. Renou, S.; Givaudan, J.G.; Poulain, S.; Dirassouyan, F.; Moulin, P. Landfill leachate treatment: Review and opportunity. *J. Hazard. Mater.* **2008**, *150*, 468–493. [[CrossRef](#)] [[PubMed](#)]
5. Kulikowska, D.; Klimiuk, E. The effect of landfill age on municipal leachate composition. *Bioresour. Technol.* **2008**, *99*, 5981–5985. [[CrossRef](#)]
6. Wijekoon, P.; Koliyabandara, P.A.; Cooray, A.T.; Su, S.L.; Athapattu, B.C.L.; Vithanage, M. Progress and prospects in mitigation of landfill leachate pollution: Risk, pollution potential, treatment and challenges. *J. Hazard. Mater.* **2022**, *421*, 126627. [[CrossRef](#)]
7. Mukherjee, S.; Mukhopadhyay, S.; Hashim, M.A.; Sen Gupta, B. Contemporary environmental issues of landfill leachate: Assessment and remedies. *Crit. Rev. Environ. Sci. Technol.* **2014**, *45*, 472–590. [[CrossRef](#)]
8. Miao, L.; Yang, G.; Tao, T.; Peng, Y. Recent advances in nitrogen removal from landfill leachate using biological treatments—A review. *J. Environ. Manag.* **2019**, *235*, 178–185. [[CrossRef](#)]
9. Foo, K.Y.; Hameed, B.H. An overview of landfill leachate treatment via activated carbon adsorption process—ScienceDirect. *J. Hazard. Mater.* **2009**, *171*, 54–60. [[CrossRef](#)]
10. Ma, S.; Zhou, C.; Pan, J.; Yang, G.; Sun, C.; Liu, Y.; Chen, X.; Zhao, Z. Leachate from municipal solid waste landfills in a global perspective: Characteristics, influential factors and environmental risks. *J. Clean. Prod.* **2021**, *333*, 130234. [[CrossRef](#)]
11. Huguët, A.; Vacher, L.; Relexans, S.; Saubusse, S.; Froidefond, J.M.; Parlanti, E. Properties of fluorescent dissolved organic matter in the gironde estuary. *Org. Geochem.* **2008**, *40*, 706–719. [[CrossRef](#)]
12. Li, J.; Zhao, L.; Qin, L.; Tian, X.; Wang, A.; Zhou, Y.; Meng, L.; Chen, Y. Removal of refractory organics in nanofiltration concentrates of municipal solid waste leachate treatment plants by combined Fenton oxidative-coagulation with photo-Fenton processes. *Chemosphere* **2016**, *146*, 442–449. [[CrossRef](#)]
13. Wang, Y.; Li, X.; Zhen, L.; Zhang, H.; Zhang, Y.; Wang, C. Electro-Fenton treatment of concentrates generated in nanofiltration of biologically pretreated landfill leachate. *J. Hazard. Mater.* **2012**, *229–230*, 115–121. [[CrossRef](#)]
14. Li, X.; Zhu, W.; Wu, Y.; Wang, C.; Zheng, J.; Xu, K.; Li, J. Recovery of potassium from landfill leachate concentrates using a combination of cation-exchange membrane electrolysis and magnesium potassium phosphate crystallization. *Sep. Purif. Technol.* **2015**, *144*, 1–7. [[CrossRef](#)]
15. Qiao, M.; Zhao, X.; Wei, X. Characterization and treatment of landfill leachate membrane concentrate by Fe²⁺/NaClO combined with advanced oxidation processes. *Sci. Rep.* **2018**, *8*, 12525. [[CrossRef](#)]
16. Labiadh, L.; Fernandes, A.; Ciriaco, L.; Pacheco, M.J.; Gadri, A.; Ammar, S.; Lopes, A. Electrochemical treatment of concentrate from reverse osmosis of sanitary landfill leachate. *J. Environ. Manag.* **2016**, *181*, 515–521. [[CrossRef](#)]
17. Hendrych, J.; Hejralova, R.; Krouzek, J.; Spacek, P.; Sobek, J. Stabilisation/solidification of landfill leachate concentrate and its residue obtained by partial evaporation. *Waste Manag.* **2019**, *95*, 560–568. [[CrossRef](#)]
18. Calabrò, P.S.; Gentili, E.; Meoni, C.; Orsi, S.; Komilis, D. Effect of the recirculation of a reverse osmosis concentrate on leachate generation: A case study in an Italian landfill. *Waste Manag.* **2018**, *76*, 643–651. [[CrossRef](#)]
19. Wu, C.; Chen, W.; Gu, Z.; Li, Q. A review of the characteristics of Fenton and ozonation systems in landfill leachate treatment—ScienceDirect. *Sci. Total Environ.* **2020**, *762*, 148557.
20. Shi, J.; Sun, D.; Dang, Y.; Qu, D. Characterizing the degradation of refractory organics from incineration leachate membrane concentrate by VUV/O₃. *Chem. Eng. J.* **2022**, *428*, 132281. [[CrossRef](#)]
21. Loh, W.; Cai, Q.; Li, R.; Jothinathan, L.; Hu, J. Reverse osmosis concentrate treatment by microbubble ozonation-biological activated carbon process: Organics removal performance and environmental impact assessment. *Sci. Total Environ.* **2021**, *798*, 149289. [[CrossRef](#)]
22. Long, Y.; Xu, J.; Shen, D.; Du, Y.; Feng, H. Effective removal of contaminants in landfill leachate membrane concentrates by coagulation. *Chemosphere* **2017**, *167*, 512–519. [[CrossRef](#)]
23. Ren, X.; Xu, X.; Xiao, Y.; Chen, W.; Song, K. Effective removal by coagulation of contaminants in concentrated leachate from municipal solid waste incineration power plants. *Sci. Total Environ.* **2019**, *685*, 392–400. [[CrossRef](#)]
24. Guo, Z.; Zhang, Y.; Jia, H.; Guo, J.; Meng, X.; Wang, J. Electrochemical methods for landfill leachate treatment: A review on electrocoagulation and electrooxidation. *Sci. Total Environ.* **2022**, *806*, 150529. [[CrossRef](#)]
25. Reshadi, M.; Bazargan, A.; McKay, G. A review of the application of adsorbents for landfill leachate treatment: Focus on magnetic adsorption. *Sci. Total Environ.* **2020**, *731*, 138863. [[CrossRef](#)]
26. Yadav, A.; Labhasetwar, P.K.; Shahi, V.K. Membrane distillation crystallization technology for zero liquid discharge and resource recovery: Opportunities, challenges and futuristic perspectives. *Sci. Total Environ.* **2022**, *806*, 150692. [[CrossRef](#)]

27. GB/T 31962-2015; Wastewater Quality Standards for Discharge to Municipal Sewers. Ministry of Housing and Urban-Rural Development of the People's Republic of China: Beijing, China, 2015.
28. Zhang, Q.-Q.; Tian, B.-H.; Zhang, X.; Ghulam, A.; Fang, C.-R.; He, R. Investigation on characteristics of leachate and concentrated leachate in three landfill leachate treatment plants. *Waste Manag.* **2013**, *11*, 2277–2286. [[CrossRef](#)]
29. Wang, H.; Wang, Y.; Li, X.; Sun, Y.; Wu, H.; Chen, D. Removal of humic substances from reverse osmosis (RO) and nanofiltration (NF) concentrated leachate using continuously ozone generation-reaction treatment equipment. *Waste Manag.* **2016**, *56*, 271–279. [[CrossRef](#)]
30. Keyikoglu, R.; Karatas, O.; Rezanian, H.; Kobya, M.; Khataee, A. A review on treatment of membrane concentrates generated from landfill leachate treatment processes. *Sep. Purif. Technol.* **2021**, *259*, 118182. [[CrossRef](#)]
31. Chen, Y.; Zhao, X.; Ye, Z.; Chen, Y.; Lin, P. Robust seawater desalination and sewage purification enabled by the solar-thermal conversion of the Janus-type graphene oxide evaporator. *Desalination* **2022**, *522*, 115406. [[CrossRef](#)]
32. Zhou, S.; Liu, X.; Zhang, K.; Shen, S. Investigation and optimization for multi-effect evaporation with thermal vapor compression (MEE-TVC) desalination system with various feed preheater arrangements. *Desalination* **2022**, *521*, 115379. [[CrossRef](#)]
33. Shi, J.; Huang, W.; Han, H.; Xu, C. Review on treatment technology of salt wastewater in coal chemical industry of China. *Desalination* **2020**, *493*, 114640. [[CrossRef](#)]
34. Ruan, G.; Wang, M.; An, Z.; Xu, G.; Ge, Y.; Zhao, H. Progress and perspectives of desalination in China. *Membranes* **2021**, *11*, 206. [[CrossRef](#)] [[PubMed](#)]
35. Al-Sahali, M.; Ettouney, H. Developments in thermal desalination processes: Design, energy, and costing aspects. *Desalination* **2007**, *214*, 227–240. [[CrossRef](#)]
36. Subramani, A.; Jacangelo, J.G. Emerging desalination technologies for water treatment: A critical review. *Water Res.* **2015**, *75*, 164–187. [[CrossRef](#)] [[PubMed](#)]
37. Qin, H.; Chen, H. Pretreatment of concentrated leachate by the combination of coagulation and catalytic ozonation with Ce/AC catalyst. *Water Sci. Technol.* **2016**, *73*, 511–519. [[CrossRef](#)] [[PubMed](#)]
38. Hao, W.; Gao, T.; Shia, W.; Zhao, M.; Huang, Z.; Ren, H.; Ruan, W. Coagulation removal of dissolved organic matter (DOM) in nanofiltration concentrate of biologically treated landfill leachate by $ZrCl_4$: Performance, mechanism and coagulant recycling. *Chemosphere* **2022**, *301*, 134768. [[CrossRef](#)] [[PubMed](#)]
39. Beijing Petrochemical Engineering Company. *Handbook of Physical and Chemical Constants for Chlor-Alkali Industry*; Chemical Industry Press: Beijing, China, 1988; Volume 7, pp. 27–30. (In Chinese)
40. Xue, X.; Lin, Z.W.; Fang, Y.M.; Zheng, F.L.; Chen, F.D.; Liu, Z.W.; Zhang, J.F. Research on the Application of “Chemical Softening + TUF + Plate-and-Frame Filtering” of Landfill Leachate in a Landfill Plant. *Technol. Water Treat.* **2022**. *in process*. Available online: <https://kns.cnki.net/kcms/detail/33.1127.P.20220630.1116.006.html> (accessed on 10 August 2021). (In Chinese)
41. Yue, D.; Xu, Y.; Bux, M.R.; Liu, F.; Nie, Y. Laboratory-scale experiments applied to the design of a two-stage submerged combustion evaporation system. *Waste Manag.* **2007**, *27*, 704–710. [[CrossRef](#)] [[PubMed](#)]
42. Tan, T.; Mai, B.; Ding, H. *Principles of Chemical Engineering*, 2nd ed.; Chemical Industry Press: Beijing, China, 1998; Volume 318. (In Chinese)
43. Liu, Y. *Alkali Recovery of Pulping Black Liquor*, 1st ed.; Chemical Industry Press: Beijing, China, 2020.
44. Liu, Y.; Pei, C.; Wang, J.; Xia, T.; Zhang, W.; Du, Y. Design and Analysis of an Evaporation System of Solutions with High Boiling Point Elevation. *Chin. J. Process Eng.* **2017**, *17*, 859–865.
45. Jiang, Y.; Zhang, G. *Glycerol Sweet Water Evaporation Calcium Sulfate Scale Cleaning and Prevention*; Shandong Chemical Industry: Jinan, China, 2013.
46. Zhang, J.; Ji, X.; Lu, W.; Chen, N. Chemical bond-parametric analysis of formation regularities of salt hydrates. *J. Shanghai Univ.* **2004**, *10*, 381–385. (In Chinese)
47. Cai, Z.; Yang, H.; Cheng, R. Hydration number of carboxylic acid ions in water. *Acta Chim. Sin.* **2008**, *66*, 831–833.
48. Li, X. *Soil Chemistry*; Higher Education Press: Beijing, China, 2001. (In Chinese)
49. He, J.; Yan, L.; Yang, K.; Ma, M.; Liu, Y.; Cui, G. Study on the composition and properties of humic acids from different source. *Chin. J. Soil Sci.* **2003**, *4*, 343–345. (In Chinese)
50. Fan, Q. Study on the Physicochemical Properties and Chemical Cohesive of Humic Acid after Radiation by UV light. Master's Thesis, Xi'an University of Architecture & Technology, Xi'an, China, 2015.
51. Jacob, B.; Waters, O.B. Calcium sulfate-sodium sulfate-sodium chloride-water system at 25° to 100°. *J. Chem. Eng. Data* **1968**, *13*, 336–344.
52. Yeatts, L.B.; Marshall, W.L. Solubility of calcium sulfate dihydrate and association equilibriums in several aqueous mixed electrolyte salt systems at 25°. *J. Chem. Eng. Data* **1972**, *17*, 163–168. [[CrossRef](#)]
53. Cameron, F.K.; Bell, J.M.; Robinson, W.O. The solubility of certain salts present in alkali soils. *J. Phys. Chem.* **1907**, *11*, 396–420. [[CrossRef](#)]
54. Paolo, V.; Renato, G. Scaling of ammonia stripping towers in the treatment of groundwater polluted by municipal solid waste landfill leachate: Study of the causes of scaling and its effects on stripping performance. *Rev. Ambiente Agua* **2015**, *10*, 240–252.
55. Luo, C.; Wen, S.; Lu, Y.; Dai, J.; Du, Y. Coprecipitation of humic acid and phosphate with Fe(III) enhances the sequestration of carbon and phosphorus in sediments. *Chem. Geol.* **2022**, *588*, 120645. [[CrossRef](#)]
56. Liu, D.Y. *Process Design Calculation and Application of Evaporator*; Chemical Industry Press: Beijing, China, 2020; pp. 18–20.

57. Zhang, L.L.; Wang, D.W.; Liu, Y.; Zhang, S.F. Calculation of coefficient of heat transfer in vapor-liquid-solid three-phase evaporator. *J. Hebei Univ. Technol.* **2011**, *40*, 41–45.
58. Liu, J.H.; Liu, H.S.; Ding, H.D. Flow boiling heat transfer to highly viscous fluid in vertical flowing. *J. Qingdao Inst. Chem. Technol.* **1995**, *16*, 118–121.